Hindawi
International Journal of Aerospace Engineering
Volume 2020, Article ID 8826968, 14 pages
https://doi.org/10.1155/2020/8826968

Research Article

Distributed Analytical Formation Control and Cooperative Guidance for Gliding Vehicles

Shengwei Jia,[1,2] Xiao Wang ,[2] Fugui Li,[2] and Yulin Wang[3]

[1]*Nanjing University of Aeronautics and Astronautics, Nanjing 210016, China*
[2]*China Academy of Launch Vehicle Technology, Beijing 100076, China*
[3]*Institute of Remote-sensing Satellite, China Academy of Space Technology, Beijing 100094, China*

Correspondence should be addressed to Xiao Wang; 2120140082@bit.edu.cn

Received 17 July 2020; Revised 6 October 2020; Accepted 24 October 2020; Published 18 November 2020

Academic Editor: Antonio Viviani

This paper addresses the analytical formation control and cooperative guidance problem for multiple hypersonic gliding vehicles under distributed communication. The gliding flight of the hypersonic gliding vehicle is divided into formation control phase and time coordination phase. In formation control phase, based on the idea of path tracking, the formation controller is designed using the second-order consensus protocol with normal positions as the coordination variables. In time coordination phase, based on the quasi-equilibrium gliding condition and the assumption of uniform deceleration motion, the analytical expression of time to go is derived. Then, the cooperative guidance method is developed using the first-order consensus protocol with time to go as the coordination variable. The proposed method takes full consideration of the characteristics of hypersonic gliding vehicle, such as complex nonlinear dynamics, no thrust, and quasi-equilibrium gliding condition, and no online numerical iteration is needed, which is well applicable for hypersonic gliding vehicles. Simulation results demonstrate the effectiveness of the formation control and cooperative guidance method.

1. Introduction

Hypersonic gliding vehicles (HGVs), which fly in the near space at the speed of over March 5 with no power, own high speed, high precision, strong maneuverability, and unpredictable trajectories, are attracting continuous attention around the world [1]. The research on trajectory design and guidance method is one of the focuses in the study of hypersonic gliding vehicles [2]. A traditional guidance method for HGVs is the nominal trajectory tracking guidance, which is derived from shuttle entry guidance and has been applied in practice successfully [3–5]. Recently, with the increasing requirements for autonomy and robustness, predictor-corrector guidance, which corrects the guidance command according to the predicting terminal error, has also been widely studied [6, 7]. On the other hand, with the successful development of HGVs, countries around the world have also conducted targeted researches on hypersonic defense weapons, including interceptors and directed energy weapons, which have greatly reduced the penetration capability and combat effectiveness of a single HGV [8]. Under this background, developing the cooperative strike technology and studying cooperative guidance for HGVs can greatly improve the penetration probability and combat effectiveness against enemy defense systems.

Cooperative guidance generally refers to the guidance method that allows multiple vehicles to fly to the target or the predetermined position at the same time. According to whether there is communication between vehicles during the flight, cooperative guidance can be divided into open-loop cooperative guidance and closed-loop cooperative guidance [9]. In open-loop cooperative guidance, which is also called time-constrained guidance, the expected time value has been determined before launching and no information interaction is needed between vehicles during the flight. Since Jeon et al. [10] first proposed a time-constrained guidance law for antiship missiles in 2006, scholars have extensively studied open-loop cooperative guidance using different methods, such as improved proportional navigation [10–12], optimal control [13, 14], sliding mode control [15–17],

trajectory shaping [18–20], and trajectory optimization [9, 21, 22]. On the other hand, closed-loop cooperative guidance can be divided into centralized cooperative guidance and distributed cooperative guidance according to the different communication modes among vehicles. In centralized cooperative guidance, there is one central node in the entire cluster that can interact with all vehicles, while in distributed cooperative guidance the vehicles in the cluster only need to exchange information with several neighbors. Centralized cooperative guidance usually designs a two-layer centralized cooperative guidance architecture based on coordination variables [23, 24]. And distributed cooperative guidance usually adopts a multiagent consensus control algorithm to deal with coordination variables [25–28]. The distributed filtering for general nonlinear systems subject to denial-of-service attacks is developed [29, 30].

However, most of the existing researches focus on the cooperative guidance for missiles and unmanned airborne vehicle (UAV) with assumptions of ideal kinematics and constant speed. For HGVs, during the entry and gliding phase, the air density changes greatly, the change range of speed is large, the vehicle dynamics change drastically, and no thrust is available [8]. Only considering the ideal kinematics of the vehicle can hardly meet the actual flight needs. Therefore, the cooperative guidance must be studied considering the characteristics of HGVs. For HGV cooperative guidance problem, Liang et al. [31] used the shooting method to optimize the longitudinal bank angle profile to meet the terminal range and height constraints, and the width of lateral heading angle corridor was iterated to meet the coordination time constraint. The adjustment capability of coordination time was further analyzed. Yu et al. [32] divided the entry trajectory into two segments. In the first segment, an angle of attack scheme was adopted, and the bank angle was iterated to satisfy the range constraint. In the second segment, the bank angle was zero, and the angle of attack was iterated to the time constraint, where the terminal speed constraint is relaxed. Fang et al. [8] trained the BP neural network offline and predicted the time to go online in real time. Then, the width of the heading angle corridor was iterated online to satisfy the time constraint and a time-constrained entry guidance method was implemented. Wang et al. [33] used a polynomial with two undetermined coefficients to design the altitude-velocity profile, and the time-constrained entry guidance was achieved by predicting the remaining range and time and correcting the two trajectory coefficients online. Then, an online cooperative guidance strategy was proposed. Base on the work of [33], Li et al. [34] studied the cooperative entry guidance with bank angle profiles. However, these cooperative guidance methods for HGVs all need online numerical iteration, which may not be practical due to the low hardware level and computing capability onboard.

Moreover, for cooperative engagement of multiple HGVs, it is necessary to consider not only the time cooperation to achieve the saturation attack on the target but also the formation flight of multiple vehicles [35]. Formation flight can effectively reduce the probability of the enemy detection system recognizing our vehicles by implementing velocity direction control and maintaining a reasonable spacing, improve the ability to resist electronic interference through the data links between vehicles to exchange information, and improve the probability of target capture and the capability of cooperative search through the cooperation of each vehicle's detection system, thereby improving overall combat effectiveness. Formation control methods for UAVs and missiles have been widely studied recently [36–38]. And they can be classified into three modes, leader-follower mode [39–41], virtual structure mode [41–43], and behavior based mode [37, 38]. However, to the authors' knowledge, there is little work about the formation control for HGVs. Besides, the formation control methods developed for UAVs are not applicable for high-speed, high-dynamic HGVs due to the following reasons. (1) In contrast to UAVs with simple kinematics, HGVs have complex and highly nonlinear dynamics, for the aerodynamic forces vary greatly with the change of flight states. (2) In contrast to UAVs where the velocity is assumed to be completely controllable, the velocity of HGV decreases monotonously in most time since the thrust is unavailable. Considering these features, the formation control for HGVs faces unique difficulties.

Motivated by above discussions, a distributed analytical formation control and cooperative guidance method aiming at the features of HGVs, such as highly nonlinear dynamics, no thrust, and quasi-equilibrium gliding condition, is proposed in this paper. The gliding flight of a HGV is divided into two phases. In the first half of gliding flight, the cooperative formation control method is studied to improve the cooperative penetration and search capability; in the second half of gliding flight, the cooperative guidance method is developed to realize time-consistency control. Aiming at the problem of formation control, a distributed formation control method is designed by taking a normal position as a coordination variable and using a multiagent consensus theory, learning from the idea of path following. The time to go is estimated analytically based on quasi-equilibrium gliding condition and uniform deceleration motion assumption. Then, a distributed cooperative guidance method is designed using consensus control algorithms without online numerical iteration. Finally, the effectiveness of formation control and cooperative guidance method is verified by numerical simulation.

The rest of this paper is organized as follows: in Section 2, the formation control and cooperative guidance problem are described. Section 3 gives the whole distributed formation control and cooperative guidance algorithm. The simulation results are presented in Section 4, and the conclusion is summarized in Section 5.

2. Problem Formulation

2.1. Equations of Motion. Ignoring the curvature and rotation of the earth, a plane rectangular coordinate system is established with the initial ground projection of any given vehicle as the origin. The Oz-axis points to the target location, and the Oy-axis is perpendicular to the local horizontal plane and points upward. The Ox-axis is set by the right-hand

relationship. Then, the relative motion of the vehicles and target is shown in Figure 1.where M_1 and M_2 represent the arbitrary two HGVs included in the vehicle cluster, respectively. In this coordinate system, the three-degree-of-freedom point-mass equations of motion of an arbitrary HGV are as follows [32]:

$$\begin{cases} \dot{x}_i = V_i \cos\theta_i \cos\psi_i, \\ \dot{y}_i = V_i \sin\theta_i, \\ \dot{z}_i = V_i \cos\theta_i \sin\psi_i, \\ \dot{V}_i = -D_i - g\sin\theta_i, \\ \dot{\theta}_i = \dfrac{L_i \cos\sigma_i}{V_i} - \dfrac{g\cos\theta_i}{V_i}, \\ \dot{\psi}_i = \dfrac{L_i \sin\sigma_i}{V_i \cos\theta_i}, \end{cases} \tag{1}$$

where V_i represents the velocity of the i-th vehicle, θ_i denotes the flight path angle, and ψ is the heading angle; g is the acceleration of gravity; σ_i represents the bank angle; L_i and D_i are the lift and drag accelerations, respectively; and L_i and D_i can be expressed as

$$\begin{cases} L_i = \dfrac{1}{2m_i}\rho_i V_i^2 C_L(\alpha_i, V_i) S_i, \\ D_i = \dfrac{1}{2m_i}\rho_i V_i^2 C_D(\alpha_i, V_i) S_i, \end{cases} \tag{2}$$

where m_i and S_i denote the mass and reference area of the i-th vehicle, respectively; α_i is the angle of attack; C_L and C_D represent the lift and drag coefficients, respectively; and ρ_i denotes the air density which can be calculated by

$$\rho_i(y_i) = 1.225 e^{-y_i/7110}. \tag{3}$$

2.2. Control Objective. The objectives of formation control and cooperative guidance in this paper are as follows.

In the first half of gliding flight, the objective is implementing velocity direction control and maintaining a reasonable spacing to improve the cooperative search capability and reduce the probability of the enemy detection system recognizing our vehicles. Therefore, it is required to design the guidance commands α_i and σ_i such that all the vehicles satisfy the following conditions:

$$\lim_{t\to\infty} \left|x_i - x_j\right| = \Delta X, \lim_{t\to\infty} \left|y_i - y_j\right| = \Delta Y, i, j = 1, 2, \cdots, n, \tag{4}$$

where ΔX and ΔY are the desired distances between two vehicles in the lateral plane and longitudinal plane in a formation configuration, respectively.

In the second half of gliding flight, the objective is achieving the cooperative guidance with time-consistency control to reach the terminal guidance handover at the same time and improve the penetration efficiency of our vehicles. It is required to design the guidance law to make all the vehicles satisfy the following conditions:

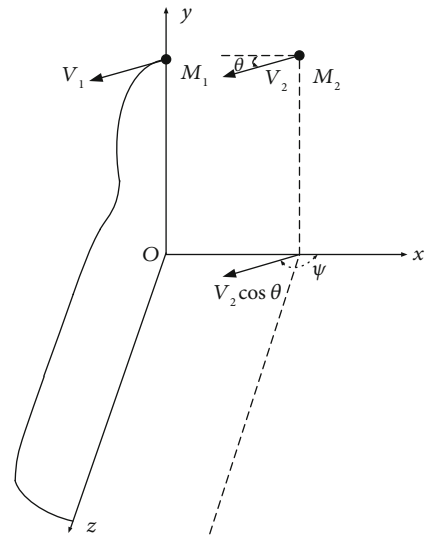

Figure 1: Formation coordinate system

$$\left|t_{f_i} - t_{f_j}\right| \le \Delta t, \quad i, j = 1, 2, \cdots, n, \tag{5}$$

where t_{f_i} is the time of arriving at the terminal guidance handover of the i-th vehicle and Δt is the allowed arrival time error.

3. Formation Control and Cooperative Guidance Law Design

In the light of whether there is communication between vehicles during the flight, cooperative guidance is classified into open-loop cooperative guidance and closed-loop cooperative guidance. And closed-loop cooperative guidance is further divided into centralized cooperative guidance and distributed cooperative guidance according to the different communication modes. The centralized cooperative guidance has the disadvantages of high communication cost, poor robustness, and difficulty in expansion. In actual application, in the event of an accident with the central node, the entire cluster will be paralyzed. Distributed communication means that the vehicle in the cluster only exchanges information with several adjacent vehicles, thereby reducing the communication cost and improving the robustness and reliability of the system. Consequently, it is of great practical significance to study distributed formation control and cooperative guidance.

In this paper, the process of distributed formation control and cooperative guidance is as follows. In the initial phase, the altitude is high, the aerodynamic control ability is weak, and each vehicle flies according to the predetermined scheme. After the altitude is gradually reduced, it turns into the formation control phase. Each vehicle calculates the guidance commands with the normal positions as the coordination variables through the consensus control algorithm

analytically, so that the normal positions tend to be consistent and the formation flight is realized. In the second half of gliding flight, which is called time coordination phase, each vehicle calculates the guidance commands with the time to go as the coordination variable analytically, so that the time to go tends to be consistent, and each vehicle finally reaches the terminal guidance handover synchronously.

3.1. Consensus Control Algorithms for Multiagent System. Firstly, the consensus control algorithms for a multiagent system are given directly without proof. It is supposed that there is a multiagent system composed of n agents that can communicate with each other [25]. The communication topology among agents in this multiagent system can be described by a directed graph $G(v, E, A)$. $v = \{v_1, v_2, \cdots, v_n\}$ is the set of nodes.$E \subseteq v \times v$ denotes a set of edges. $A = [a_{ij}] \in \mathbb{R}^{n\times n}$ denotes the weighted adjacency matrix of G, where $a_{ij} = 1$ denotes that agent i can receive information from agent j and $a_{ij} = 0 (i \neq j)$ denotes that agent i cannot receive information from agent j. $L = [l_{ij}] \in \mathbb{R}^{n\times n}$ is the Laplacian matrix of G, where

$$l_{ij} = \begin{cases} \sum_{k=1,k\neq i}^{n} a_{ik}, i = j, \\ -a_{ij}, i \neq j. \end{cases} \tag{6}$$

Then, the following lemmas are given directly.

Lemma 1 [27, 44]. *Consider a first-order multiagent system (7),*

$$\dot{x}_i = u_i, \quad i = 1, 2, \cdots, n, \tag{7}$$

where x_i is the agent state and u_i is the control input. If the consensus protocol is designed as

$$u_i = -\sum_{j=1}^{n} a_{ij}(x_i - x_j), \quad i, j = 1, 2, \cdots, n, \tag{8}$$

the system states can achieve consensus asymptotically, that is,

$$\lim_{t\to\infty} |x_i - x_j| = 0, \quad i, j = 1, 2, \cdots, n. \tag{9}$$

If the consensus protocol is designed as

$$u_i = -\sum_{j=1}^{n} a_{ij}(x_i - x_j) - \xi(x_i - x_d), \quad i, j = 1, 2, \cdots, n, \tag{10}$$

where $\xi > 0$ is the control gain and x_d is the desired state. The system states can asymptotically converge to x_d, that is,

$$\lim_{t\to\infty} |x_i - x_d| = 0, \quad i = 1, 2, \cdots, n. \tag{11}$$

Lemma 2 [27, 44]. *Consider a second-order multiagent system (12),*

$$\begin{cases} \dot{x}_i = v_i, \\ \dot{v}_i = u_i, i = 1, 2, \cdots, n, \end{cases} \tag{12}$$

where x_i and v_i are the agent states and u_i is the control input. If the consensus protocol is designed as

$$u_i = -\sum_{j=1}^{n} a_{ij}(x_i - x_j) - \gamma \sum_{j=1}^{n} a_{ij}(v_i - v_j), i, j = 1, 2, \cdots, n, \tag{13}$$

where $\gamma > 0$ is the control gain. The system states can achieve consensus asymptotically, that is,

$$\lim_{t\to\infty} |x_i - x_j| = 0, \lim_{t\to\infty} |v_i - v_j| = 0, i, j = 1, 2, \cdots, n. \tag{14}$$

If the consensus protocol is designed as

$$\begin{aligned} u_i = &-\sum_{j=1}^{n} a_{ij}(x_i - x_j) - \gamma \sum_{j=1}^{n} a_{ij}(v_i - v_j) \\ &- \xi(v_i - v_d), i, j = 1, 2, \cdots, n, \end{aligned} \tag{15}$$

where v_d is the desired state. Then, x_i can achieve consensus asymptotically and v_i can asymptotically converge to v_d, that is,

$$\lim_{t\to\infty} |x_i - x_j| = 0, \lim_{t\to\infty} |v_i - v_d| = 0, i, j = 1, 2, \cdots, n. \tag{16}$$

3.2. Formation Control Law Design. For distributed formation control, in the initial phase, the aerodynamic capability of each vehicle is weak, so the scheme of the angle of attack and bank angle can be given beforehand and the vehicle flies according to the scheme. After entering the formation control phase, if the three position variables are directly controlled and the control variables are the angle of attack and bank angle, the formation control problem will be an underactuated problem and is difficult to deal with, because there is no thrust. Since the purpose of formation control phase is to control the velocity direction and spacing of HGVs, the flight time and speed are not strictly required. With reference to the idea of path tracking in trajectory tracking [45], only the normal motions are controlled to make the normal motions consistent, and the formation function of velocity direction control and reasonable spacing can be achieved.

First, considering the lateral plane, the coordination variable can be chosen as $\bar{x}_i = x_i + \Delta x_i$, where$\Delta x_i$ is a constant distance of the i-th vehicle in the formation. When coordination variables are consistent, we can obtain $\bar{x}_i = \bar{x}_j$ and $x_i - x_j = \Delta x_j - \Delta x_i$, that is, the lateral distance maintained between the two vehicles is $\Delta x_j - \Delta x_i$. The first derivative and second derivative versus time of $\bar{x}_i$ can be calculated by

$$\begin{aligned} \dot{\bar{x}}_i &= V_i \cos\theta_i \cos\psi_i, \\ \ddot{\bar{x}}_i &= -D_i \cos\theta_i \cos\psi_i - L_i \sin\sigma_i \sin\psi_i - L_i \cos\sigma_i \sin\theta_i \cos\psi_i. \end{aligned} \tag{17}$$

Using the consensus protocol (13) to design the control law for lateral plane,

$$\begin{aligned} &-D_i \cos\theta_i \cos\psi_i - L_i \sin\sigma_i \sin\psi_i - L_i \cos\sigma_i \sin\theta_i \cos\psi_i \\ &\quad = -K_1 \sum_{j=1}^{n} a_{ij}\left(\bar{x}_i - \bar{x}_j\right) - K_2 \sum_{j=1}^{n} a_{ij}\left(\dot{\bar{x}}_i - \dot{\bar{x}}_j\right), \end{aligned} \tag{18}$$

where $K_1, K_2 > 0$ are the control gains. Under the control law (18), $\bar{x}_i$ and $\dot{\bar{x}}_i$ can achieve consensus asymptotically and lateral formation is formed.

Then, considering the longitudinal plane, the coordination variable is chosen as $\bar{y}_i = y_i + \Delta y_i$, where$\Delta y_i$ is a constant distance. When coordination variables are consistent, we can get $\bar{y}_i = \bar{y}_j$ and $y_i - y_j = \Delta y_j - \Delta y_i$; that is, the longitudinal distance maintained between the two vehicles is$\Delta y_j - \Delta y_i$. The first derivative and second derivative versus time of $\bar{x}_i$ can be derived by

$$\begin{aligned} \dot{\bar{y}}_i &= V_i \sin\theta_i, \\ \ddot{\bar{y}}_i &= -D_i \sin\theta_i - g + L_i \cos\sigma_i \cos\theta_i. \end{aligned} \tag{19}$$

Using the consensus protocol (15) to design the control law for longitudinal plane,

$$\begin{aligned} &-D_i \sin\theta_i - g + L_i \cos\sigma_i \cos\theta_i \\ &\quad = -K_1 \sum_{j=1}^{n} a_{ij}\left(\bar{y}_i - \bar{y}_j\right) - K_2 \sum_{j=1}^{n} a_{ij}\left(\dot{\bar{y}}_i - \dot{\bar{y}}_j\right) - \xi\left(\dot{\bar{y}}_i - \dot{y}_d\right), \end{aligned} \tag{20}$$

where $\dot{y}_d$ is the desired change rate of altitude of a HGV. Under the control law (20), $\bar{y}_i$ can achieve consensus asymptotically and $\dot{\bar{y}}_i$ can asymptotically converge to $\dot{y}_d$.

The actual control inputs in formation are the angle of attack α_i and bank angle σ_i. α_i and σ_i are implicit in the terms D_i, $L_i \cos\sigma_i$, $L_i \sin\sigma_i$ in the left side of equations (18) and (20). In other words, equations (18) and (20) are nonlinear functions of two independent variables about α_i and σ_i. However, equations (18) and (20) cannot be solved analytically and it is too complicated using numerical methods. To this end, we design the following solution process. First, calculate the drag accelerations D_i using the angle of attack α_i of the last guidance cycle. Then, $L_i \cos\sigma_i$ can be solved in the equation (20) with the calculated D_i. After that, D_i and $L_i \cos\sigma_i$ are known in equation (18), and $L_i \sin\sigma_i$ can be derived. Finally, according to the following BTT-180 control logic [46], we can obtain L_i and σ_i. Using the current states of the vehicle, the lift coefficient C_L can be inversely calculated, and then, the angle of attack α_i can be calculated according to the aerodynamic model.

$$\begin{aligned} L_i &= \sqrt{(L_i \cos\sigma_i)^2 + (L_i \sin\sigma_i)^2}, \\ \sigma_i &= \begin{cases} \arctan\left(\dfrac{L_i \sin\sigma_i}{L_i \cos\sigma_i}\right), & \text{if } L_i \cos\sigma_i > 0, \\ \operatorname{sgn}(L_i \sin\sigma_i)\left(\dfrac{\pi}{2}\right), & \text{if } L_i \cos\sigma_i = 0, \\ \arctan\left(\dfrac{L_i \sin\sigma_i}{L_i \cos\sigma_i}\right) + \operatorname{sgn}(L_i \sin\sigma_i)\pi, & \text{if } L_i \cos\sigma_i < 0,\ L_i \sin\sigma_i \neq 0, \\ \pi, & \text{if } L_i \cos\sigma_i < 0,\ L_i \sin\sigma_i = 0, \end{cases} \\ \alpha_i &= C_L^{-1}\left(\frac{2m_i L_i}{\rho_i V_i^2 S_i}\right). \end{aligned} \tag{21}$$

In each guidance cycle, D_i is updated in real time, and the above steps are repeated to calculate the guidance commands α_i and σ_i. The error caused by using the angle of attack α_i of the last guidance cycle will be gradually eliminated in the continuous updating.

Remark 1. The idea of path tracking is adopted in this section, and only the normal motion is controlled to reduce the dimension of formation control. Then, the formation function of velocity direction control and reasonable spacing can also be realized. Besides, the point-mass dynamics and the change of velocity are considered, which is distinctly different from existing formation control methods for UAVs.

Remark 2. In the control law (20), the term $\dot{y}_d$ makes the HGV maintain a constant descent rate in formation and satisfy quasi-equilibrium gliding condition without oscillations. Therefore, this formation control law conforms better to the dynamic characteristics of HGVs.

3.3. Cooperative Guidance Law Design. The phase from the end of formation control phase to the handover of terminal guidance is the time coordination phase. In this phase, a distributed analytical cooperative guidance law is designed to make all the vehicles reach the terminal guidance handover at the same time, thus improving the penetration efficiency of the cluster.

It is assumed that the quasi-equilibrium gliding condition is satisfied in HGVs during the flight. Quasi-equilibrium gliding condition (QEGC) means that the change rate of the flight path angle is zero and flight path angle is a constant, that is $\dot{\theta}_i = 0$ and $\theta_i = \text{const}$ [2]. Under QEGC, we have

$$\dot{\theta}_i = L_i \cos\sigma_i - g \cos\theta_i = 0. \tag{22}$$

Considering the flight path angle is rather small and close to zero, $\cos\theta_i \approx 1$ is obtained. Then, we get

$$L_i \cos\sigma_i = g, \tag{23}$$

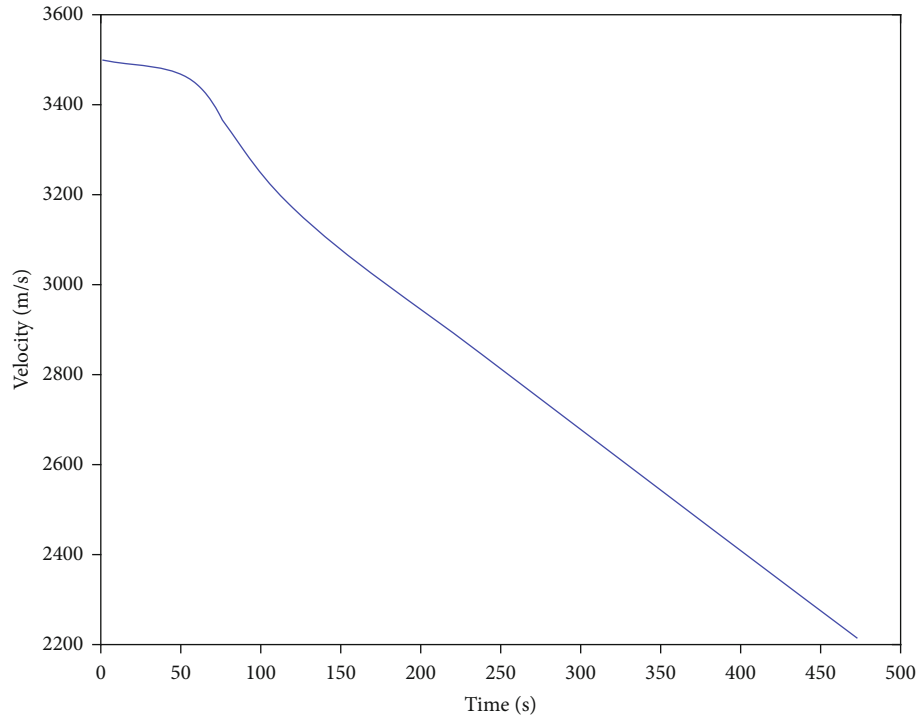

Figure 2: The velocity curve of a HGV.

which implies that the component of lift force in the longitudinal plane is balanced with gravity. According to equation (1), the change rate of velocity is derived as

$$\begin{aligned}\dot{V}_i &= -D_i - g\sin\theta_i, = -L_i\frac{C_D}{C_L} - g\sin\theta_i,\\ &= -\frac{C_D}{C_L\cos\sigma_i}g - g\sin\theta_i.\end{aligned} \tag{24}$$

When the angle of attack does not change much, the lift-to-drag ratio of the HGV is approximately constant. When the lateral maneuver of the HGV is small, $\cos\sigma_i \approx 1$. In addition, $\sin\theta_i$ is constant under QEGC. Then, according to equation (24), the acceleration $\dot{V}_i$ can be assumed a constant.

Furthermore, simulation analysis is carried out. Figures 2 and 3 are the velocity curve and acceleration curve of a HGV, respectively. As shown in the figures, the HGV satisfies QEGC, and the velocity decreases linearly and the acceleration is close to a constant value after stabilization. The simulation result is consistent with the theoretical analysis. Therefore, it can be assumed that the vehicle flies with uniform deceleration in the range direction (z direction). According to the formula of uniform deceleration motion,

$$s_{\mathrm{go}_i} = V_{0_i}t_{\mathrm{go}_i} + \frac{1}{2}a_i t_{\mathrm{go}_i}^2, \tag{25}$$

where s_{go_i} is the range to go, $V_{0_i} = V_i\cos\theta_i$ is the horizontal velocity, t_{go_i} is the time to go, and$a_i = \dot{V}_{0_i}$ is the acceleration. And the terminal time is $t_{f_i} = t_i + t_{\mathrm{go}_i}$. Using equation (25), we can estimate the time to go analytically according to the current acceleration

$$t_{\mathrm{go}_i} = \frac{-V_{0_i} + \sqrt{V_{0_i}^2 + 2a_i s_{\mathrm{go}_i}}}{a_i}. \tag{26}$$

In order to realize the distributed control of the time to go, t_{go_i} is chosen as the coordination variable, and the time derivative of t_{go_i} is calculated as

$$\begin{aligned}\dot{s}_{\mathrm{go}_i} &= V_{0_i}\dot{t}_{\mathrm{go}_i} + a_i t_{\mathrm{go}_i} + \frac{1}{2}\dot{a}_i t_{\mathrm{go}_i}^2 + a_i\dot{t}_{\mathrm{go}_i}t_{\mathrm{go}_i}, -V_{0_i}\\ &= \dot{t}_{\mathrm{go}_i}\left(V_{0_i} + a_i t_{\mathrm{go}_i}\right) + a_i t_{\mathrm{go}_i} + \frac{1}{2}\dot{a}_i t_{\mathrm{go}_i}^2, \dot{t}_{\mathrm{go}_i}\\ &= -1 - \frac{\dot{a}_i t_{\mathrm{go}_i}^2}{2\left(V_{0_i} + a_i t_{\mathrm{go}_i}\right)},\end{aligned} \tag{27}$$

where $a_i = \dot{V}_{0_i} = (V_i\cos\theta_i)'$. Under QEGC, the flight path angle is rather small and close to zero, and$\cos\theta_i \approx 1, \sin\theta_i \approx 0$. Thus, we have

$$a_i = \dot{V}_{0_i} = (V_i\cos\theta_i)' \approx \dot{V}_i = (-D_i - g\sin\theta_i)' \approx -\dot{D}_i. \tag{28}$$

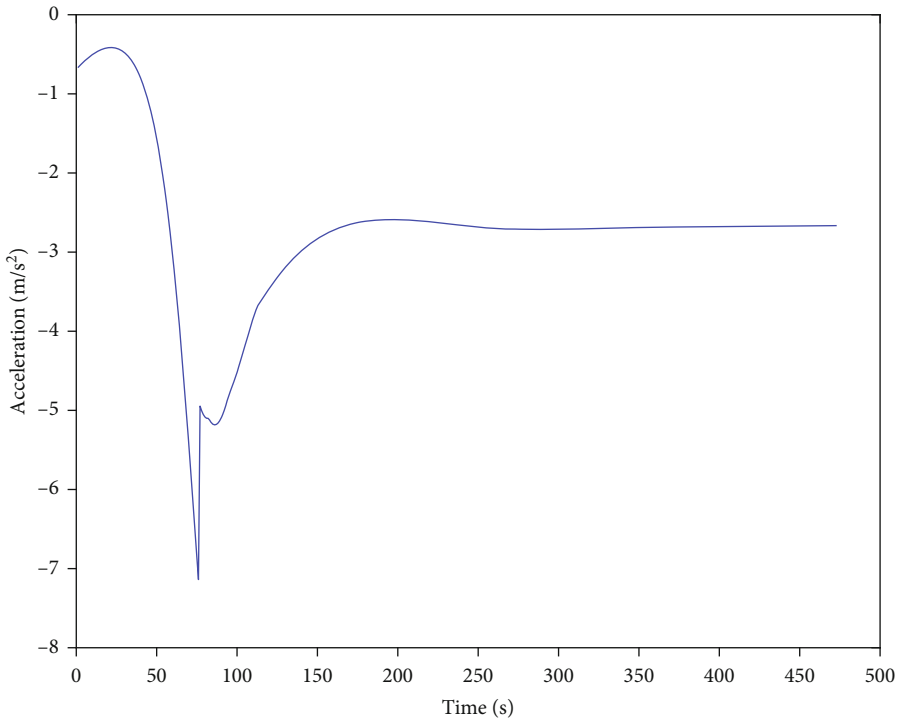

Figure 3: The acceleration curve of a HGV.

The formula of $-\dot{D}_i$ is further deduced.

$$-\dot{D}_i = -\frac{S_i}{2m_i}\left(\dot{\rho}_i V_i^2 C_D + 2\rho_i V_i \dot{V}_i C_D + \rho_i V_i^2 \frac{\partial C_D}{\partial \alpha}\dot{\alpha}_i\right). \quad (29)$$

Substituting equations (28) and (29) into (27), we obtain

$$\dot{t}_{go_i} = -1 + \frac{S_i t_{go_i}^2}{4m_i\left(V_{0_i} + a_i t_{go_i}\right)} \cdot \left(\dot{\rho}_i V_i^2 C_D + 2\rho_i V_i \dot{V}_i C_D + \rho_i V_i^2 \frac{\partial C_D}{\partial \alpha}\dot{\alpha}_i\right). \quad (30)$$

In equation (30), the change rate of angle of attack $\dot{\alpha}_i$ is chosen as the control input. Then, the dynamic equation of time to go t_{go_i} is calculated by

$$\dot{t}_{go_i} = F + G\dot{\alpha}_i, \quad (31)$$

where $F = -1 + (S_i t_{go_i}^2/(4m_i(V_{0_i} + a_i t_{go_i})))(\dot{\rho}_i V_i^2 C_D + 2\rho_i V_i \dot{V}_i C_D)$ and $G = (\rho_i V_i^2 S_i t_{go_i}^2/(4m_i(V_{0_i} + a_i t_{go_i})))(\partial C_D/\partial\alpha)$.

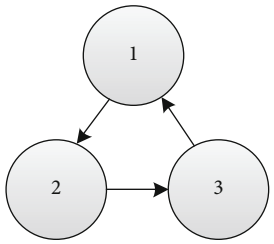

Figure 4: The communication topology for three HGVs.

Using the consensus protocol (10) to design the distributed control law for time to go,

$$\dot{\alpha}_i = \frac{\left[-\sum_{j=1}^{n} a_{ij}\left(t_{go_i} - t_{go_j}\right) - \xi\left(t_{go_i} - t_{go_d}\right) - F\right]}{G}, \quad (32)$$

where $t_{go_d} = t_{f_d} - t$ is the desired time to go and t_{f_d} is the desired terminal time. The term t_{go_d} in the control law (32) can make the terminal times of vehicles converge to the desired terminal time consistently and avoid the divergence of the control law.

It is noted that although the control input is the change rate of angle of attack $\dot{\alpha}$ in equation (31), the guidance command that the guidance system outputs to the attitude control system is still the angle of attack α in practical application. Therefore, the real guidance command α should

Table 1: The initial states of three vehicles.

Vehicle	x (km)	y (km)	z (km)	V (m/s)	θ (°)	ψ (°)
Vehicle 1	0	60	0	3500	0	90
Vehicle 2	4	61	0	3510	0	90
Vehicle 3	-4	59	0	3520	0	90

Table 2: Two different formation configurations.

Configuration	Vehicle 1	Vehicle 2	Vehicle 3
Case 1	$\Delta x_1 = 0$ km, $\Delta y_1 = 0$ km	$\Delta x_2 = 2$ km, $\Delta y_2 = 0$ km	$\Delta x_3 = -2$ km, $\Delta y_2 = 0$ km
Case 2	$\Delta x_1 = 0$ km, $\Delta y_1 = 0$ km	$\Delta x_2 = 1$ km, $\Delta y_2 = -1$ km	$\Delta x_3 = -1$ km, $\Delta y_2 = -1$ km

be calculated by integrating $\dot{\alpha}$ in real time. In addition, to avoid the frequent changes of the angle of attack, no guidance command is updated and $\dot{\alpha}_i = 0$ when $|t_{go_i} - t_{go_j}| < 1$ ($j = 1, 2, \cdots, n$).

The above control of time to go is based on longitudinal motion. For lateral motion, to make the lateral states consistent, the lateral control law is still adopted as (18). The difference is that the angle of attack α has been decided in longitudinal motion and D_i, L_i are fixed. Then, according to equation (18), we obtain

$$\begin{aligned} &-D_i \cos\theta_i \cos\psi_i - L_i \sin\sigma_i \sin\psi_i - L_i \cos\sigma_i \sin\theta_i \cos\psi_i \\ &\quad = -K_1 \sum_{j=1}^{n} a_{ij}\left(\bar{x}_i - \bar{x}_j\right) - K_2 \sum_{j=1}^{n} a_{ij}\left(\dot{\bar{x}}_i - \dot{\bar{x}}_j\right), \sin\sigma_i \sin\psi_i \\ &\qquad + \cos\sigma_i \sin\theta_i \cos\psi_i = \Theta, \end{aligned}$$

$$\Theta = \frac{K_1 \sum_{j=1}^{n} a_{ij}\left(\bar{x}_i - \bar{x}_j\right) + K_2 \sum_{j=1}^{n} a_{ij}\left(\dot{\bar{x}}_i - \dot{\bar{x}}_j\right) - D_i \cos\theta_i \cos\psi_i}{L_i}. \tag{33}$$

Merging equation (33), we can get

$$\sqrt{\sin^2\psi_i + \sin^2\theta_i \cos^2\psi_i}\, \sin\left[\sigma_i + \arctan\left(\frac{\sin\theta_i}{\tan\psi_i}\right)\right] = \Theta, \tag{34}$$

where $(\sin\theta_i/\tan\psi_i) \approx 0$. Then, the command of bank angle is solved

$$\sigma_i = \arcsin \frac{K_1 \sum_{j=1}^{n} a_{ij}\left(\bar{x}_i - \bar{x}_j\right) + K_2 \sum_{j=1}^{n} a_{ij}\left(\dot{\bar{x}}_i - \dot{\bar{x}}_j\right) - D_i \cos\theta_i \cos\psi_i}{L_i \sqrt{\sin^2\psi_i + \sin^2\theta_i \cos^2\psi_i}}. \tag{35}$$

In summary, in time coordination phase, the command of the angle of attack is calculated for each vehicle according to control law (32) to make the time to go consistent, and all vehicles reach the terminal guidance handover at the same time. The command of bank angle is solved according to control law (35) to make lateral motion consistent.

Remark 3. Generally, the amplitude of lateral motion of a HGV is far less than the amplitude in the range direction. Therefore, the influence of lateral control law (35) on control of time to go can be ignored.

Remark 4. The approximations and simplifications by QEGC, constant lift-to-drag ratio, and uniform deceleration motion when the guidance law is derived will cause control errors in one guidance cycle. However, the errors will be continuously corrected during online guidance.

Remark 5. The formation control laws (18) and (20) and cooperative guidance laws (32) and (35) are all analytical forms, and no numerical iteration is needed.

Therefore, the online computing burden is much lower than existing cooperative guidance methods [8, 31–34].

4. Simulation Results

In this section, simulations are carried out to illustrate the effectiveness of the proposed formation control and cooperative guidance scheme. The CAV-H [47] is adopted as the simulation model. Considering the scenario of formation and cooperative flight with three HGVs, the distributed communication topology for three HGVs is shown in Figure 4.

The initial states of three vehicles are shown in Table 1.

BTT-180 control mode is adopted, and the constraints for control variables are $0 \le \alpha \le 25°$, $|\sigma| \le 180°$. The flight phase is set as follows. The first 75 s is the initial phase. 75 s to 320 s is the formation control phase. From 320 s to terminal guidance, handover is the time coordination phase. The terminal guidance handover is when the vehicle is 150 km from the target. The position of target is 0, 0, and 1600 km.

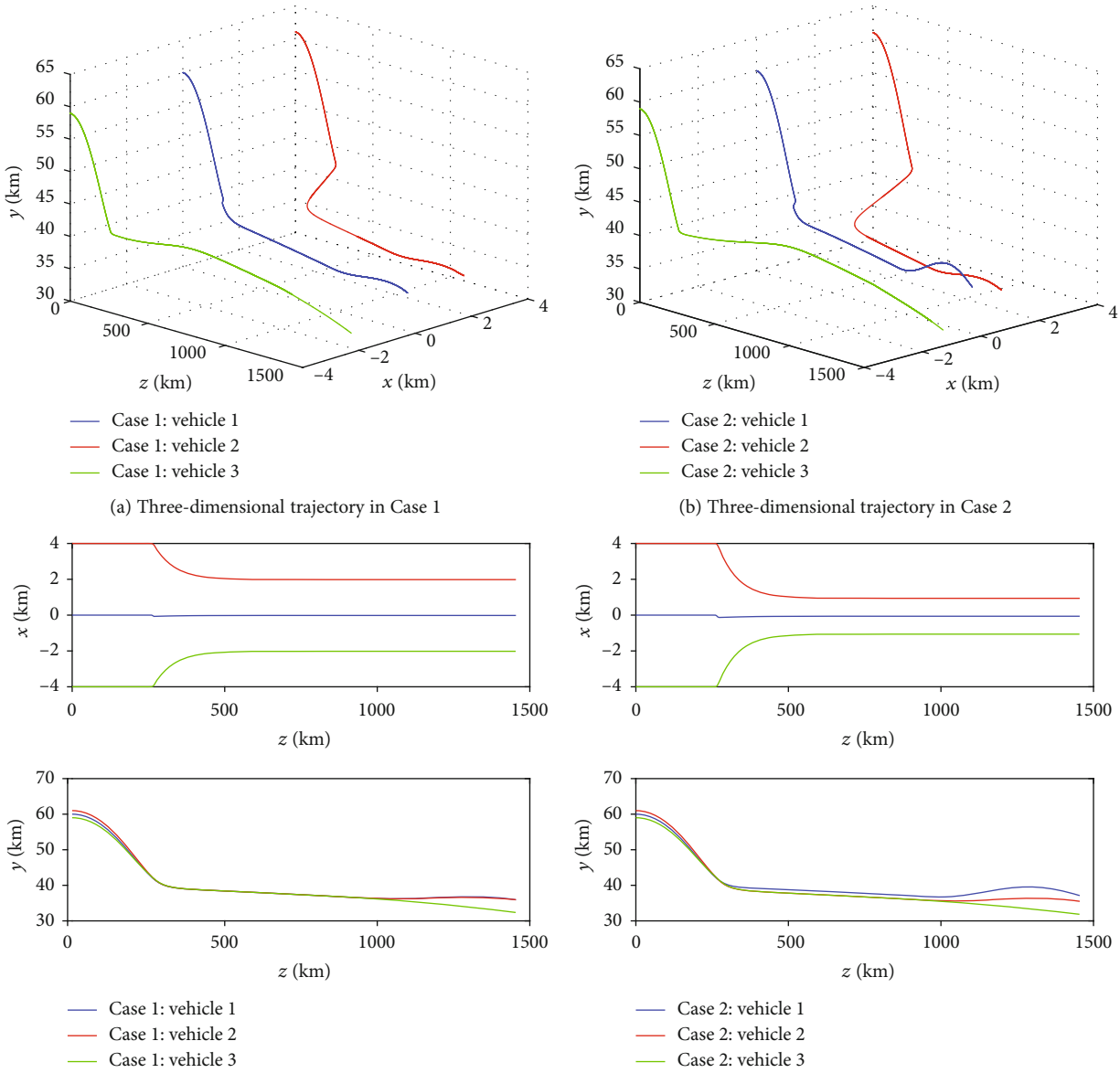

(a) Three-dimensional trajectory in Case 1

(b) Three-dimensional trajectory in Case 2

(c) Two-dimensional trajectory in Case 1

(d) Two-dimensional trajectory in Case 2

Figure 5: Continued.

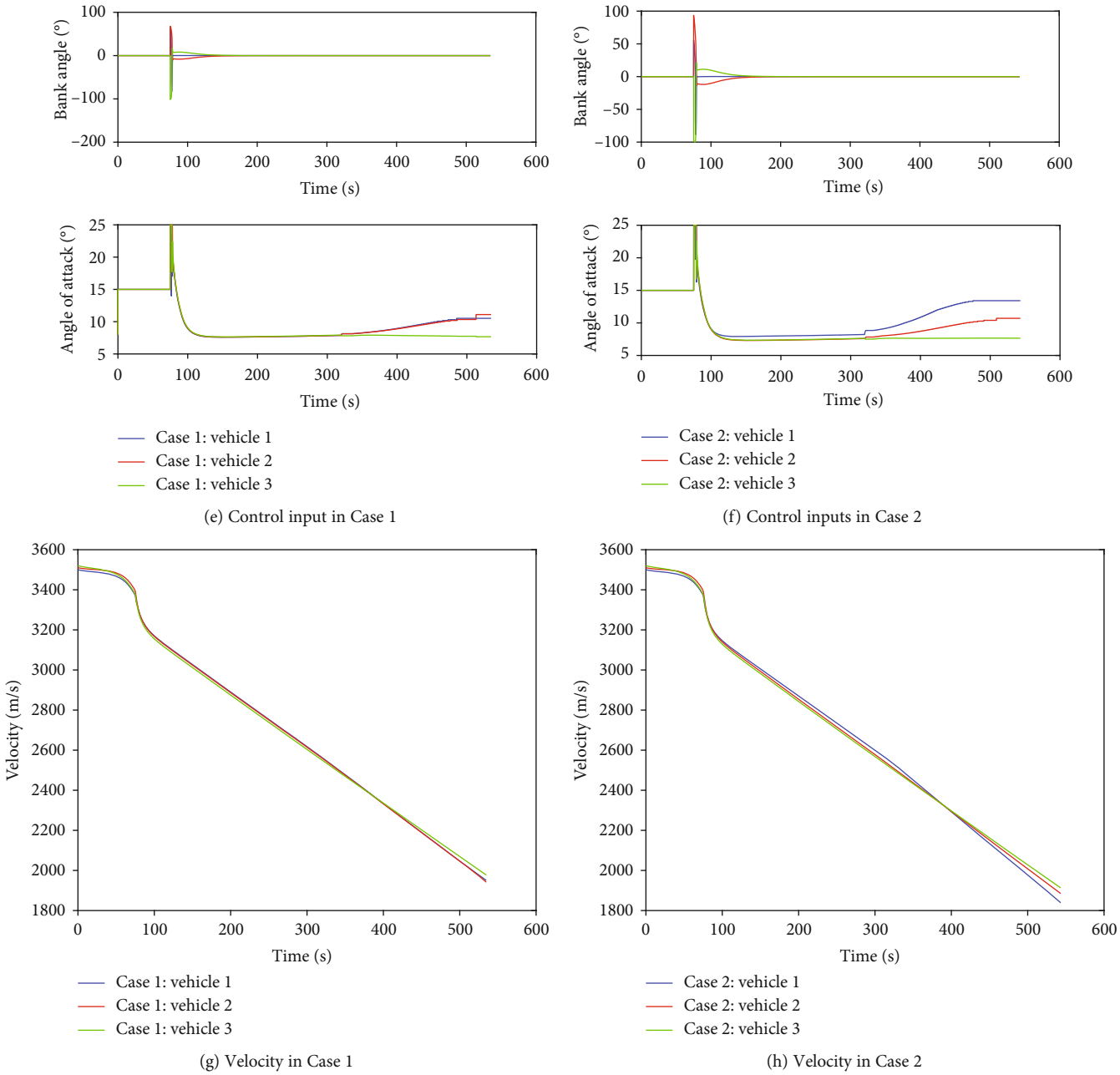

(e) Control input in Case 1

(f) Control inputs in Case 2

(g) Velocity in Case 1

(h) Velocity in Case 2

Figure 5: Simulation results of different formation configurations.

Table 3: Terminal times of different formation configurations.

Configurations	Vehicle 1	Vehicle 2	Vehicle 3
Case 1	534.8s	534.7s	534.7s
Case 2	543.2s	543.6s	543.6s

The scheme of angle of attack and bank angle in initial phase is set as follows:

$$\begin{cases} \alpha = 15^{\circ}, \\ \sigma = 0^{\circ}, t < 75s. \end{cases} \tag{36}$$

The termination condition of simulation for each vehicle is when the vehicle is 150 km from the target.

4.1. Simulations with Different Formation Configurations. In this section, two different formation configurations are considered, as shown in Table 2. In Case 1, the three vehicles are at the same horizontal plane. Vehicle 1 is in the middle, Vehicle 2 is in the right, and Vehicle 3 is in the left. The horizontal spacing is 2 km. In Case 2, the configuration of three vehicles is like a triangular shape. Vehicle 2 and Vehicle 3 are 1 km lower than Vehicle 1. The horizontal spacing is 1 km.

It can be seen from Figure 5 and Table 3 that the two formation configurations can be both realized well with

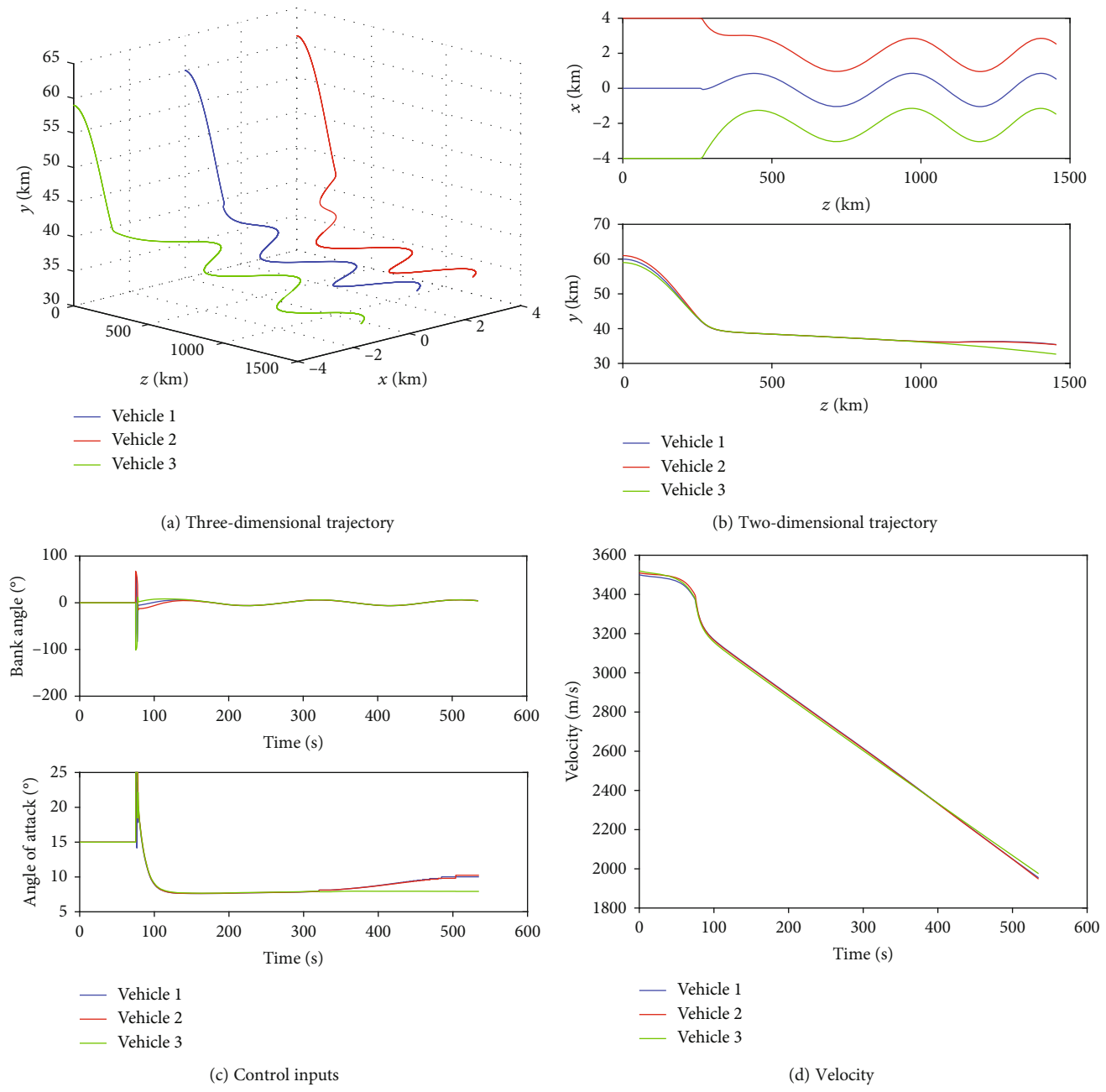

Figure 6: Simulation results of lateral maneuver.

Table 4: Terminal times of lateral maneuver.

Vehicle	Vehicle 1	Vehicle 2	Vehicle 3
Terminal time	535.2s	535.1s	534.9s

the proposed formation control method. In the first half of gliding flight, which is the formation control phase, the commands of the angle of attack and bank angle are calculated by consensus control algorithms, thus bringing about the consistency control of coordination variables. In Case 2, the angles of attack of Vehicle 2 and Vehicle 3 are less than the one of Vehicle 1, because Vehicle 2 and Vehicle 3 fly lower than Vehicle 1 in formation configuration. The results also show that the longitudinal trajectory of each vehicle is smooth, achieving a stable descent and satisfying QEGC. In the second half of gliding flight, which is the time coordination phase, each vehicle can decelerate properly by adjusting the command of angle of attack, so as to achieve the consistency control of time to go, and the terminal time errors are less than 1 s in Table 3. The lateral maneuver exists, and the bank angle is not zero only when the formation is formed. There is no lateral maneuver at other times, and the bank angles are all zero.

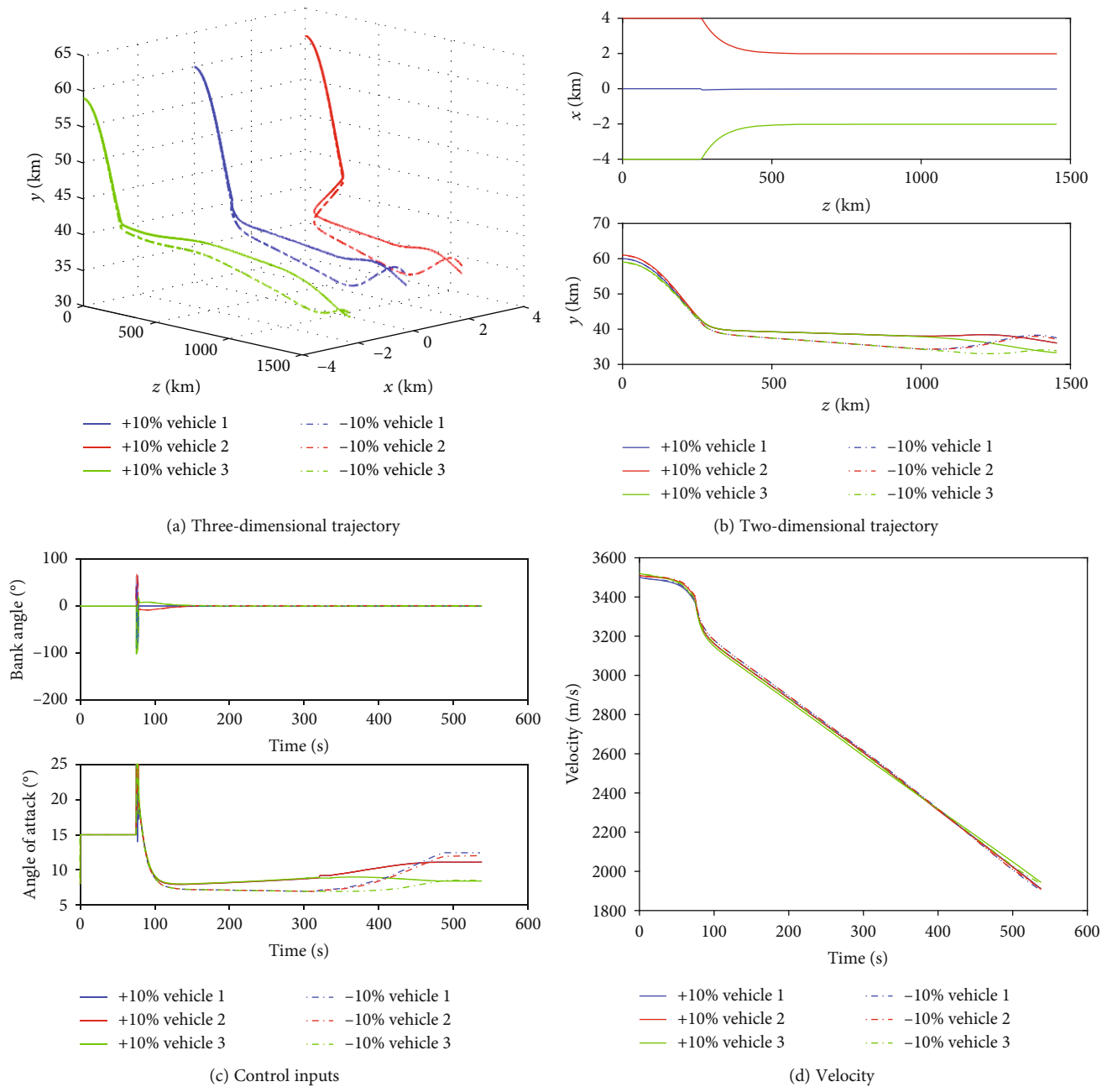

Figure 7: Simulation results of aerodynamic parameter perturbations.

4.2. Simulations with Lateral Maneuver. In this section, to increase the penetration probability, the lateral sinusoidal maneuver is considered. The formation configuration is the same as Case 1 in Section 4.1. To realize the lateral sinusoidal maneuver, the control law (18) for lateral plane is changed into

$$-D_i \cos\theta_i \cos\psi_i - L_i \sin\sigma_i \sin\psi_i - L_i \cos\sigma_i \sin\theta_i \cos\psi_i = -K_1 \sum_{j=1}^{n} a_{ij}\left(\bar{x}_i - \bar{x}_j\right) - K_2 \sum_{j=1}^{n} a_{ij}\left(\dot{\bar{x}}_i - \dot{\bar{x}}_j\right) - \xi\left(\dot{\bar{x}}_i - \dot{x}_d\right), \tag{37}$$

where $\dot{x}_d = A_m \omega \cos\left[\omega(t-75) + \varphi_0\right]$ is the desired change rate of x direction, $A_m = 1$ km is the lateral maneuver amplitude, $\omega = 0.0333$ rad/s is the maneuver frequency, and $\varphi_0 = 0^\circ$ is the initial phase.

As shown in Figure 6 and Table 4, the formation configuration with lateral maneuver can also be realized with the proposed formation control method. The longitudinal trajectory of each vehicle is smooth, achieving a stable descent, while the lateral trajectory presents a sinusoidal shape. When the formation is stable, each vehicle still needs a certain bank angle to provide lateral overload to maintain lateral maneuver. However, due to the small amplitude of lateral maneuver designed, it has little effect

Table 5: Terminal times of aerodynamic parameter perturbations.

Perturbations	Vehicle 1	Vehicle 2	Vehicle 3
+10%	538.3s	538.3s	538.1s
−10%	537.0s	537.2s	537.1s

on the overall longitudinal motion. If the designed lateral maneuver is very large, the penetration probability can be increased, but the range capability of the vehicle will be greatly reduced. Therefore, some trade-offs should be made.

4.3. Simulations with Parameter Perturbations. The formation control and cooperative guidance with aerodynamic parameter perturbation are further considered in this section. The formation configuration is the same as Case 1 in Section 4.1. Consider the cases of aerodynamic parameter perturbation +10% and −10%, respectively.

As seen in Figure 7 and Table 5, the formation control and cooperative guidance with aerodynamic parameter perturbations can be achieved with the proposed method. The longitudinal trajectory of each vehicle is smooth and decreases steadily. When the aerodynamic parameters increase, the formation trajectory is higher. This is because when the lift coefficient increases, in order to keep the lift constant to balance gravity, the dynamic pressure must be reduced. When the flight altitude increases, the density decreases and the corresponding dynamic pressure decreases. On the contrary, when the aerodynamic parameters decrease, the formation trajectory becomes lower.

5. Conclusion

In this paper, a distributed formation control and cooperative guidance method in analytical form is proposed considering the dynamic characteristics of HGVs. The gliding flight of a HGV is divided into formation control phase and time coordination phase. In formation control phase, the formation controller is designed using the second-order consensus protocol with the normal positions as the coordination variables. In time coordination phase, the expression of time to go is deduced and the analytical cooperative guidance law is studied using the first-order consensus protocol with the times to go as the coordination variables. In contrast to traditional formation control methods for missiles and UAVs, the high-speed and high-dynamic model with no thrust is taken into account. Compared to traditional cooperative guidance methods for HGVs, the analytical guidance command is given and no online numerical iteration is needed. Simulation results show that the proposed method can achieve different functions of formation control and time coordination with robustness, which can be applied to HGVs. Besides, in distributed communication architecture, the consumption of communication resource is less with strong robustness and reliability.

Data Availability

The data used to support the findings of this study are available from the corresponding author upon request.

Conflicts of Interest

We declare that there is no conflict of interest in this paper.

References

[1] H. Stephens, "Near-space," *Air Force Magazine*, vol. 88, no. 7, pp. 36–40, 2005.

[2] Z. Shen and P. Lu, "Onboard generation of three-dimensional constrained entry trajectories," *Journal of Guidance, Control, and Dynamics*, vol. 26, no. 1, pp. 111–121, 2003.

[3] J. C. Harpold and C. A. Graves, "Shuttle entry guidance," *Journal of the Astronautical Sciences*, vol. 27, no. 3, pp. 239–268, 1979.

[4] J. Guo, X. Wu, and S. Tang, "Autonomous gliding entry guidance with geographic constraints," *Chinese Journal of Aeronautics*, vol. 28, no. 5, pp. 1343–1354, 2015.

[5] X. Wang, J. Guo, S. Tang, S. Qi, and Z. Wang, "Entry trajectory planning with terminal full states constraints and multiple geographic constraints," *Aerospace Science and Technology*, vol. 84, pp. 620–631, 2019.

[6] S. Xue and P. Lu, "Constrained predictor-corrector entry guidance," *Journal of Guidance, Control, and Dynamics*, vol. 33, no. 4, pp. 1273–1281, 2010.

[7] P. Lu, "Entry guidance: a unified method," *Journal of Guidance, Control, and Dynamics*, vol. 37, no. 3, pp. 713–728, 2014.

[8] K. Fang, Q. Z. Zhang, K. Ni, L. Cheng, and Y. T. Huang, "Time-coordination reentry guidance law of hypersonic vehicle," *Acta Aeronautica et Astronautica Sinica*, vol. 39, no. 5, pp. 202–217, 2018.

[9] W. Dong, Q. Wen, Q. Xia, and S. Yang, "Multiple-constraint cooperative guidance based on two-stage sequential convex programming," *Chinese Journal of Aeronautics*, vol. 33, no. 1, pp. 296–307, 2020.

[10] I. S. Jeon, J. I. Lee, and M. J. Tahk, "Impact-time-control guidance law for anti-ship missiles," *IEEE Transactions on Control Systems Technology*, vol. 14, no. 2, pp. 260–266, 2006.

[11] I. S. Jeon, J. I. Lee, and M. J. Tahk, "Impact-time-control guidance with generalized proportional navigation based on nonlinear formulation," *Journal of Guidance, Control, and Dynamics*, vol. 39, no. 8, pp. 1887–1892, 2016.

[12] J. I. Lee, I. S. Jeon, and M. J. Tahk, "Guidance law to control impact time and angle," *IEEE Transactions on Aerospace and Electronic Systems*, vol. 43, no. 1, pp. 301–310, 2007.

[13] X. Chen and J. Wang, "Optimal control based guidance law to control both impact time and impact angle," *Aerospace Science and Technology*, vol. 84, pp. 454–463, 2019.

[14] S. He and D. Lin, "Three-dimensional optimal impact time guidance for antiship missiles," *Journal of Guidance, Control, and Dynamics*, vol. 42, no. 4, pp. 941–948, 2019.

[15] N. Harl and S. N. Balakrishnan, "Impact time and angle guidance with sliding mode control," *IEEE Transactions on Control Systems Technology*, vol. 20, no. 6, pp. 1436–1449, 2012.

[16] S. R. Kumar and D. Ghose, "Impact time guidance for large heading errors using sliding mode control," *IEEE Transactions*

on Aerospace and Electronic Systems, vol. 51, no. 4, pp. 3123–3138, 2015.

[17] A. Sinha and S. R. Kumar, "Super-twisting control based impact time constrained guidance," in *AIAA Scitech 2020 Forum*, Orlando, Florida, 2020.

[18] R. Livermore, R. Tsalik, and T. Shima, "Elliptic Guidance," *Journal of Guidance, Control, and Dynamics*, vol. 41, no. 11, pp. 2435–2444, 2018.

[19] R. Tsalik and T. Shima, "Circular impact-time guidance," *Journal of Guidance, Control, and Dynamics*, vol. 42, no. 8, pp. 1836–1847, 2019.

[20] X. Yan, J. Zhu, M. Kuang, and X. Yuan, "A computational-geometry-based 3-dimensional guidance law to control impact time and angle," *Aerospace Science and Technology*, vol. 98, article 105672, Article ID 105672, 2020.

[21] H. Jiang, Z. An, Y.'. Yu, S. Chen, and F. F. Xiong, "Cooperative guidance with multiple constraints using convex optimization," *Aerospace Science and Technology*, vol. 79, pp. 426–440, 2018.

[22] B. Pan, Y. Ma, and R. Yan, "Newton-type methods in computational guidance," *Journal of Guidance, Control, and Dynamics*, vol. 42, no. 2, pp. 377–383, 2019.

[23] J. Zhao, R. Zhou, and Z. Dong, "Three-dimensional cooperative guidance laws against stationary and maneuvering targets," *Chinese Journal of Aeronautics*, vol. 28, no. 4, pp. 1104–1120, 2015.

[24] X. Wang, Y. Zhang, D. Liu, and M. He, "Three-dimensional cooperative guidance and control law for multiple reentry missiles with time-varying velocities," *Aerospace Science and Technology*, vol. 80, pp. 127–143, 2018.

[25] T. Lyu, Y. Guo, C. Li, G. Ma, and H. Zhang, "Multiple missiles cooperative guidance with simultaneous attack requirement under directed topologies," *Aerospace Science and Technology*, vol. 89, pp. 100–110, 2019.

[26] S. Kang, J. Wang, G. Li, J. Shan, and I. R. Petersen, "Optimal cooperative guidance law for salvo attack: an MPC-based consensus perspective," *IEEE Transactions on Aerospace and Electronic Systems*, vol. 54, no. 5, pp. 2397–2410, 2018.

[27] S. He, W. Wang, D. Lin, and H. Lei, "Consensus-based two-stage salvo attack guidance," *IEEE Transactions on Aerospace and Electronic Systems*, vol. 54, no. 3, pp. 1555–1566, 2018.

[28] Y. Chen, J. Wang, C. Wang, J. Shan, and M. Xin, "Three-dimensional cooperative homing guidance law with field-of-view constraint," *Journal of Guidance, Control, and Dynamics*, vol. 43, no. 2, pp. 389–397, 2020.

[29] W. Chen, D. Ding, H. Dong, and G. Wei, "Distributed resilient filtering for power systems subject to denial-of-service attacks," *IEEE Transactions on Systems, Man, and Cybernetics: Systems*, vol. 49, no. 8, pp. 1688–1697, 2019.

[30] D. Ding, Z. Wang, and Q. L. Han, "A set-membership approach to event-triggered filtering for general nonlinear systems over sensor networks," *IEEE Transactions on Automatic Control*, vol. 65, no. 4, pp. 1792–1799, 2020.

[31] Z. Liang, J. Yu, Z. Ren, and Q. Li, "Trajectory planning for cooperative flight of two hypersonic entry vehicles," in *21st AIAA International Space Planes and Hypersonics Technologies Conference*, Xiamen, China, 2017.

[32] J. Yu, X. Dong, Q. Li, Z. Ren, and J. Lv, "Cooperative guidance strategy for multiple hypersonic gliding vehicles system," *Chinese Journal of Aeronautics*, vol. 33, no. 3, pp. 990–1005, 2020.

[33] W. Xiao, G. Jie, T. Shengjing, and Q. Shuai, "Time-cooperative entry guidance based on analytic profile," *Acta Aeronautica et Astronautica Sinica*, vol. 40, no. 3, pp. 239–250, 2019.

[34] Z. Li, B. He, M. Wang, H. Lin, and X. An, "Time-coordination entry guidance for multi-hypersonic vehicles," *Aerospace Science and Technology*, vol. 89, pp. 123–135, 2019.

[35] W. Yu, Y. Yao, and W. Chen, "Analytical cooperative entry guidance for rendezvous and formation flight," *Acta Astronautica*, vol. 171, pp. 118–138, 2020.

[36] J. Yu, X. Dong, Q. Li, and Z. Ren, "Cooperative integrated practical time-varying formation tracking and control for multiple missiles system," *Aerospace Science and Technology*, vol. 93, article 105300, 2019.

[37] X. K. Wang, X. Li, and Z. Q. Zheng, "Survey of developments on multi-agent formation control related problems[J]," *Control and decision*, vol. 28, no. 11, pp. 1601–1613, 2013.

[38] K. K. Oh, M. C. Park, and H. S. Ahn, "A survey of multi-agent formation control," *Automatica*, vol. 53, pp. 424–440, 2015.

[39] N. Cui, C. Wei, J. Guo, and B. Zhao, "Research on missile formation control system," in *2009 International Conference on Mechatronics and Automation*, pp. 4197–4202, Changchun, China, 2009.

[40] X. Jin and W. M. Haddad, "An adaptive control architecture for leader–follower multiagent systems with stochastic disturbances and sensor and actuator attacks," *International Journal of Control*, vol. 92, no. 11, pp. 2561–2570, 2019.

[41] C. Wei, Y. Shen, X. Ma, J. Guo, and N. Cui, "Optimal formation keeping control in missile cooperative engagement," *Aircraft Engineering and Aerospace Technology*, vol. 84, no. 6, pp. 376–389, 2012.

[42] Y. Y. An and S. Q. Li, "Study of multiple robotic fishes formation strategy based on behavior planning method," *Computer Simulation*, vol. 11, p. 84, 2013.

[43] S. Ahmad, Z. Feng, and G. Hu, "Multi-robot formation control using distributed null space behavioral approach," in *2014 IEEE International Conference on Robotics and Automation (ICRA)*, pp. 3607–3612, Hong Kong, China, 2014.

[44] W. Ren, R. W. Beard, and E. M. Atkins, "A survey of consensus problems in multi-agent coordination," in *Proceedings of the 2005, American Control Conference, 2005*, pp. 1859–1864, Portland, OR, USA, USA, 2005.

[45] A. P. Aguiar and J. P. Hespanha, "Trajectory-tracking and path-following of underactuated autonomous vehicles with parametric modeling uncertainty," *IEEE Transactions on Automatic Control*, vol. 52, no. 8, pp. 1362–1379, 2007.

[46] L. C. Shen, S. C. Peng, Y. F. Niu, W. M. Sun, and L. Pan, "A survey on guidance laws for BTT missiles," *Journal of National University of Defense Technology*, vol. 33, no. 2, pp. 106–112, 2011.

[47] T. H. Phillips, "A common aero vehicle (CAV) model, description, and employment guide," *Schafer Corporation for AFRL and AFSPC*, vol. 27, 2003.